Transactions on Electrical and Electronic Materials (2018) 19:101–105
https://doi.org/10.1007/s42341-018-0015-y

Online ISSN 2092-7592
Print ISSN 1229-7607

REGULAR PAPER

Dislocation-Related Electron Transport in Au Schottky Junctions on AlGaN/GaN

Hogyoung Kim[1] · Keun Man Song[2]

Received: 6 January 2017 / Revised: 19 December 2017 / Accepted: 3 January 2018 / Published online: 27 February 2018

Abstract
We investigated the electrical properties of Au/AlGaN/GaN Schottky junctions as a function of temperature by analyzing the current–voltage (*I–V*) measurements. The barrier height increased with increasing temperature, but the ideality factor decreased. Increases in temperature are associated with barrier inhomogeneity. The modified Richardson plots for $Al_{0.25}Ga_{0.75}N$ yielded a higher Richardson constant, 77.3 A $cm^{-2}K^{-2}$, than theoretically predicted (30.0 A cm^{-2} K^{-2}). This indicates that the thermionic emission (TE) model with barrier inhomogeneity is not suitable for explaining the transport characteristics of the junction. We fitted the experimental *I–V* data to predictions based on various transport mechanisms, such as TE, generation-recombination, and tunneling currents. The dominant transport mechanism at all temperatures was found to be caused by the tunneling current. The dislocation model of the tunneling current yielded a dislocation density of 2.96×10^6 cm^{-2}.

Keywords AlGaN/GaN · Tunneling current · Dislocation density

1 Introduction

Among III–V-compound-based devices, much attention has been devoted to the study of AlGaN/GaN heterostructure field-effect transistors (HEMTs) because of their applications in high-frequency, high-temperature, and high-voltage electronic devices [1, 2]. We can improve the performance and reliability of these devices by using AlGaN with a large Schottky barrier height (SBH), as this decreases the leakage current and increases the breakdown voltage [3]. The excessive reverse leakage current is a critical challenge limiting the applicability of AlGaN/GaN HEMTs. This increases the low frequency noise, causes current collapse, and lowers the breakdown voltage [4]. Several investigations have been conducted to explain the current transport mechanisms for reverse leakage current [5, 6]. For example, Yan et al. [5] showed that the reverse gate leakage in AlGaN/GaN can be analyzed in terms of a Poole–Frenkel (PF) emission mechanism with a trap-assisted process. Liu et al. [6] investigated the transport mechanism of the forward gate current in Al_2O_3/AlGaN/GaN metal–oxide–semiconductor HEMTs (MOS-HEMTs), and found the dominant transport mechanisms at low and high temperatures to be Fowler–Nordheim (F-N) tunneling and trap-assisted tunneling (TAT), respectively. These studies focused on low-Al-composition AlGaN. Zhu et al. [7] investigated the transport mechanisms governing gate leakage currents in $Al_2O_3/Al_{0.55}Ga_{0.45}N$/GaN structures.

The results of investigations into the SBHs of Au, Ni and Re on AlGaN, based on current–voltage (*I–V*) and capacitance–voltage (*C–V*) measurements, suggest that the relationship between the barrier height and the Al mole fraction is linear [8–10]. By assuming that the electron affinity on x for $Al_xGa_{1-x}N$ (χ_{GaN} = 4.2 eV and χ_{AlN} = 2.05 eV) varies linearly with the work function of Ni (5.15 eV), Qiao et al. [8] found the barrier height of a sample with $x = 0.23$ to be lower than expected. This may have been caused by the high density of interface states. Such problems are inevitable because the lattice mismatch and the difference between the thermal expansion coefficients of the (In, Al)GaN film and sapphire substrate are both significant.

✉ Hogyoung Kim
hogyoungkim@gmail.com

[1] Department of Visual Optics, Seoul National University of Science and Technology (Seoultech), Seoul 01811, South Korea

[2] Korea Advanced Nano Fab Center, Suwon, Gyeonggi 16229, South Korea

The current-transport mechanisms in metal–semiconductor (MS) and metal–insulator semiconductor (MIS) diodes depend on a variety of parameters, such as the surface preparation process, formation of insulating layers between the metal and semiconductor, barrier height inhomogeneity, concentration of impurities in the semiconductor, density of interface states or defects, and series resistance of the device [11]. We cannot obtain detailed information about the electron conduction process at the metal/semiconductor interface if we only measure the *I–V* characteristics of MS, MIS, and solar cells at room temperature. In this study, we investigated the temperature-dependent electrical properties of a Au/$Al_{0.25}Ga_{0.75}$/GaN Schottky diode with respect to a range of possible transport mechanisms.

2 Experiments

The AlGaN/GaN thin films used in this study were grown on a *c*-plane (0001) sapphire substrate by metal–organic chemical vapor deposition (MOCVD). The layer structure consisted of a conventional low-temperature GaN buffer layer, followed by a 3-μm-thick unintentionally doped (undoped) GaN and a 200-nm-thick $Al_{0.25}Ga_{0.75}N$ film. Trimethylgallium (TMGa) and ammonia (NH_3) were used as group III and group V precursors, respectively. According to Hall-effect measurements at room temperature, the sheet carrier concentration was 2.3×10^{13} cm^{-2}. We used electron beam evaporation to prepare the Schottky contacts by depositing 50-nm-thick Au films through a shadow mask with exposed diameters of 300, 500, and 700 μm. A 150-nm-thick layer of Al metal was deposited to serve as the ohmic contact. We took *I–V* measurements at various temperatures using a Keithley 238 current source in conjunction with a hot chuck connected to a temperature controller.

3 Results and Discussion

Figure 1a shows the linear *I–V* curves measured at room temperature, which exhibit the rectifying characteristics. The semilogarithmic *I–V* curves shown on the inset indicate that the reverse leakage current increases rapidly. This might be due to the interface states. We used the thermionic emission (TE) model to determine the SBH (ϕ_B) and ideality factor (n) from the linear regions of the ln(I)–V curves under forward bias for values of V greater than $3kT/q$. We followed the method suggested by Qiao et al. [8] to calculate the theoretical effective Richardson constant A^*, where $A^* = 2\pi qm^*k^2/h^3$, h is Plank's constant, and m^* is the effective mass of electrons in AlGaN. The Richardson constant of $Al_{0.25}Ga_{0.75}N$ was calculated to be approximately 30.0 A $cm^{-2}K^{-2}$ and the effective barrier height and

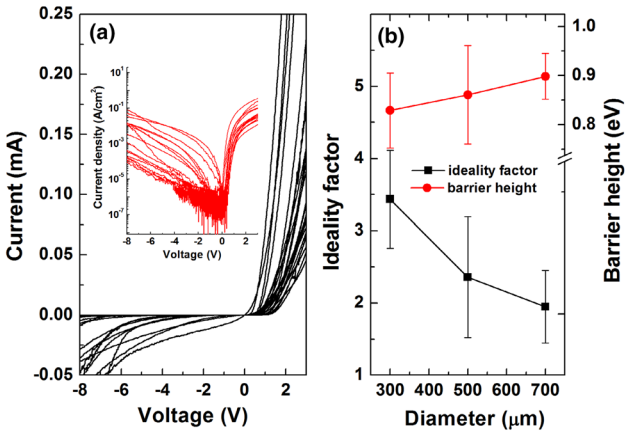

Fig. 1 The linear current–voltage (*I–V*) characteristics, extracted ideality factor, and effective barrier height for different contact areas. The inset in **a** presents the semilogarithmic *I–V* characteristics

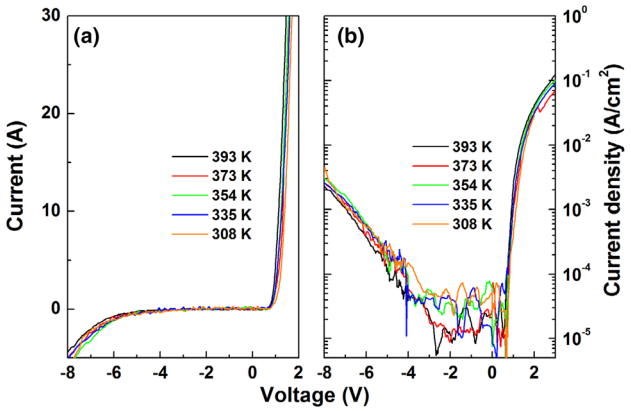

Fig. 2 **a** Linear and **b** semilogarithmic *I–V* curves measured at various temperatures

ideality factor were determined to be 0.86 (± 0.08) and 2.54 (± 0.91), respectively. We then analyzed these values in terms of the contact area, as shown in Fig. 1b. The barrier height increased with the contact area, but the ideality factor decreased. In Au/n-Ge contacts, it has been shown that the contribution of the tunneling current toward the total current increases as the contact area decreases [12]. Larger tunneling currents can increase the ideality factor and decrease the barrier height [13]. Hence, the passivation layer around the periphery of the contact can improve device reliability.

We investigated the current transport in more detail by taking temperature-dependent *I–V* measurements. Figure 2a shows the linear *I–V* curves measured at various temperatures. The diode exhibited rectifying characteristics at all temperatures. Figure 2b shows that the reverse leakage current started to increase rapidly when the voltage increased beyond − 4 V. We were able to infer the temperature dependence of the ideality factor and the barrier height from the

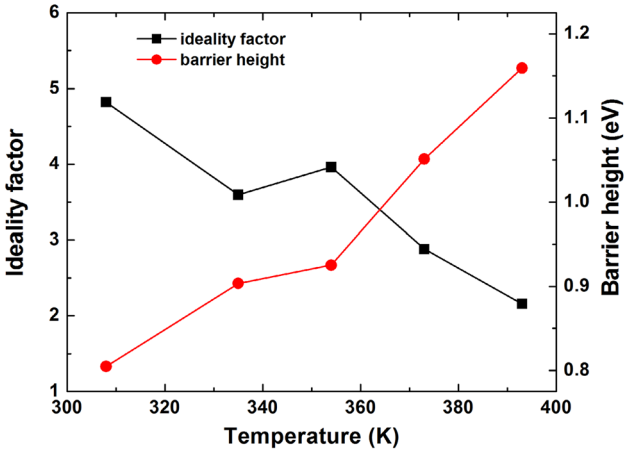

Fig. 3 Ideality factor and barrier height as a function of temperature

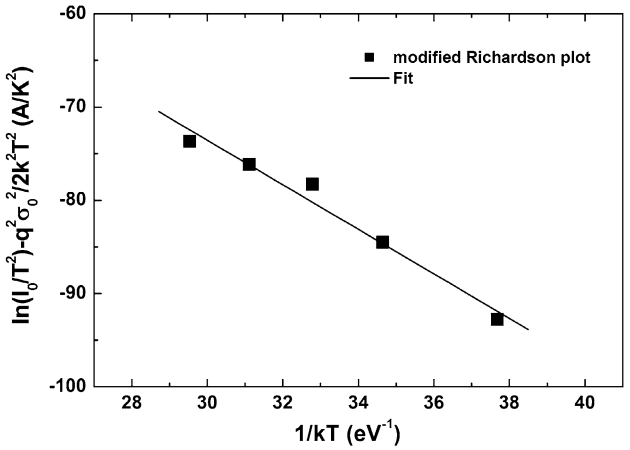

Fig. 4 Modified Richardson plot of $\ln(I_0/T^2)$–$q^2\sigma_0^2/2k^2T^2$ versus $1/kT$

I–V measurements, as shown in Fig. 3. The barrier height increased as the temperature increased, but the ideality factor decreased. The barrier height and ideality factor have often been observed to vary in this manner as the temperature of real Schottky diodes increases. This is thought to be due to lateral variations in the barrier height [13]. We obtained a higher value for the ideality factor at 308 K than previously reported [14, 15]. It is possible that the ideality factor increased as a result of high series resistance.

The temperature dependent barrier height can be expressed as $\phi_B = \bar{\phi}_B - q\sigma_0^2/2kT$, where $\bar{\phi}_B$ is the zero-bias mean barrier height and σ_0 is the standard deviation. If we take the lateral barrier inhomogeneity into account, we can calculate the modified Richardson plot as follows:

$$\ln(I_0/T^2) - q^2\sigma_0^2/2k^2T^2 = \ln(AA^*) - q\bar{\phi}_B/kT, \quad (1)$$

where I_0 is the reverse bias saturation current and A is the contact area. Figure 4 shows plots of $\ln(I_0/T^2) - q^2\sigma_0^2/2k^2T^2$ versus $1/kT$.

The intercepts at the ordinate produced a modified Richardson constant of 77.3 A $cm^{-2}K^{-2}$. This value is higher than the theoretical value of 30.0 A $cm^{-2}K^{-2}$ for $Al_{0.25}Ga_{0.75}N$. Moreover, the zero-bias mean barrier height was found to be approximately 2.34 eV, which is too large. Therefore, the current transport properties of the Au/AlGaN Schottky contacts cannot be explained in terms of the TE model with barrier inhomogeneity.

We conducted a detailed analysis of the current transport mechanisms for the forward bias *I–V* characteristics in terms of various components of the electron transport: TE current (I_{TE}), generation-recombination current (I_{GR}), tunneling current (I_{TU}) and leakage current (I_{LE}) [11, 16]. We assumed that the total current I_{TOT} ($I_{TOT} = I_{TE} + I_{GR} + I_{TU} + I_{LE}$) could be calculated by calculating the sum of all of these component currents. The TE current is

$$I_{TE} = I_{TE0}[\exp\{q(V - IR_S)/kT\} - 1], \quad (2)$$

where I_{TE0} is the saturation current of the TE component and R_S is the series resistance. Here, I_{TE0} is given by

$$I_{TE0} = AA^*T^2 \exp(-\Phi_B/kT), \quad (3)$$

where Φ_B is the barrier height. The GR current is

$$I_{GR} = I_{GR0}[\exp\{q(V - IR_S)/2kT\} - 1], \quad (4)$$

where I_{GR0} is the saturation current of the GR component. The tunneling current is

$$I_{TU} = I_{TU0}[\exp\{q(V - IR_S)/E_t\} - 1], \quad (5)$$

where I_{TU0} is the saturation current of the tunneling component and E_t is the tunneling energy. The leakage current is

$$I_{LE} = (V - IR_S)/R_{Sh}, \quad (6)$$

where R_{Sh} is the shunt resistance, which can be approximated from the reverse *I–V* characteristics of the diodes. As we found the contribution of the LE current to be negligible at all temperatures, we omitted it from the subsequent analysis. We fitted the experimental forward bias *I–V* data to theoretical *I–V* curves for all temperatures measured by taking I_{TE0}, I_{TU0}, and E_0 as fitting parameters. For example, Fig. 5 shows a comparison between the experimental and fitted curves at 393 K. We also fitted the combinations of the TE, GR, and tunneling currents to the experimental *I–V* data at all temperatures. The contribution from the TE current became more important as the bias voltage increased. However, the transport was dominated by the contribution from the tunneling current over the entire bias region. The fitting results were similar at the other temperatures.

We used Eq. (2) to calculate the barrier heights from the I_{TE0} values of the TE component at each temperature, as shown in Fig. 6a. The barrier heights exhibited a very weak temperature dependence (average value of 1.79 eV). The temperature coefficient of the linear model of the data was slightly negative, which is consistent with the theoretical

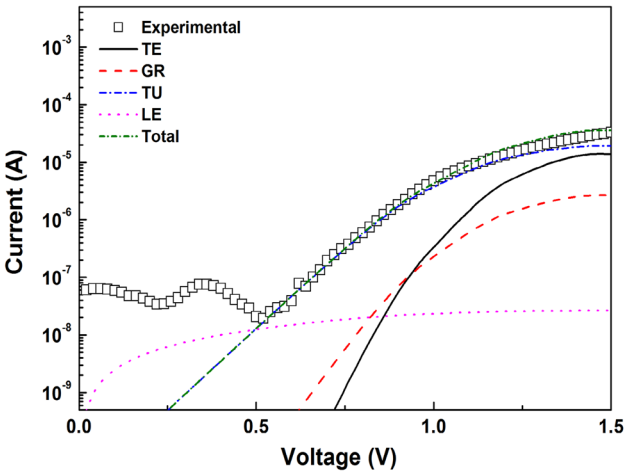

Fig. 5 Fitting results of the forward *I–V* characteristics of Au/AlGaN/GaN Schottky junctions

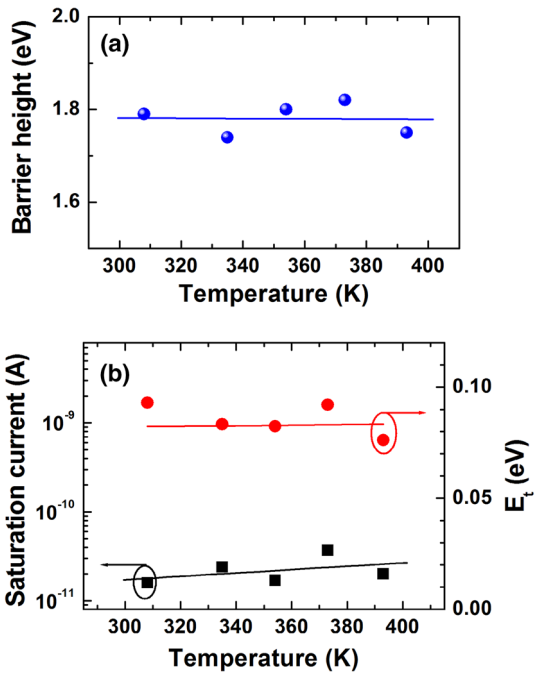

Fig. 6 **a** Barrier height and **b** tunneling saturation current and tunneling energy as a function of temperature

prediction. As $\Phi_B \cong E_g/3$, the barrier heights are roughly related to the band gap energy [16]. Hence, according to the E_g versus x dependence, we expected the barrier height to be 1.31 eV when the Al mole fraction is $x = 0.25$ [8]. This value is lower than the barrier heights presented in Fig. 6a. However, Monroy et al. [17] investigated Au/AlGaN photodiodes and found the barrier height to be about 1.75 eV for an Al mole fraction of $x = 0.25$. Similarly, a barrier height of 1.72 eV was reported in the case of Ni/Au Schottky diodes on $Al_{0.27}Ga_{0.73}N$/GaN [18]. This implies that our analysis, which incorporates various transport mechanisms, explains the forward *I–V* characteristics of the Au/AlGaN/GaN Schottky diode well.

According to the dislocation model of the tunneling current, the tunneling saturation current I_{TU0} at 0 K can be expressed as [16]

$$I_{TU0} = qAv_D N_{dis} \exp(-\Phi_B/E_t), \quad (7)$$

where v_d (~ 1.5×10^{13} s^{-1} [19]) is the Debye frequency and N_{dis} is the dislocation density. Figure 6b shows the tunneling saturation current, I_{TU0}, and the barrier energy, E_t, as functions of temperature. The tunneling saturation current increased (although not significantly) as the temperature increased, whereas the variations in the tunneling energy were very small. We extrapolated the linear fitting to the data presented in Fig. 6b to 0 K to obtain I_{TU0} and E_t, which were 4.6×10^{-12} A and 0.082 eV, respectively. Finally, we used Eq. (7) to calculate the dislocation density. Our value, 2.96×10^6 cm^{-2}, was very similar to the values reported by Arslan et al. [11] (2.4×10^6 cm^{-2}) and Ren et al. [18] (8.8×10^6 cm^{-2}). These results indicate that the dislocation-related tunneling current is the dominant current transport mechanism in Au/AlGaN/GaN Schottky diodes. It has been reported that abnormally high leakage currents in n-type GaN can be explained by a thin surface barrier (TSB) model. According to this model, the presence of unintentional surface donors reduces the width of the Schottky barrier so that carriers can tunnel the potential barrier easily [20]. Hence, both the dislocation and surface defects may contribute to tunneling in AlGaN-based devices.

4 Conclusions

The temperature-dependent electrical properties of Au/AlGaN/GaN Schottky diodes were investigated using *I–V* measurements. Taking into account barrier inhomogeneity, modified Richardson plots yielded a Richardson constant of 77.3 A $cm^{-2}K^{-2}$, which is higher than the theoretical value of 30.0 A $cm^{-2}K^{-2}$ for $Al_{0.25}Ga_{0.75}N$. We then fitted the experimental *I–V* data to the results predicted by various transport mechanisms to obtain a detailed understanding of the transport mechanisms. According to our analysis, the tunneling current dominates the transport at all of the measured temperatures. We used a theoretical model of the dislocation-related tunneling current to obtain a value for the dislocation density, which was 2.96×10^6 cm^{-2}.

Acknowledgemenst This research was supported in part by the Basic Science Research Program through the National Research Foundation of Korea (NRF) funded by the Ministry of Education (2017R1D1A1B03030400).

References

1. J. Ibbetson, P. Fini, K. Ness, S. DenBaars, J. Speck, U. Mishra, Appl. Phys. Lett. **77**, 250 (2000). https://doi.org/10.1063/1.126940
2. O. Ambacher, J. Smart, J. Shealy, N. Weimann, K. Chu, M. Murphy, W. Schaffl, L. Eastman, R. Dimitrov, L. Wittmer, M. Stutzmann, W. Rieger, J. Hilsenbeck, J. Appl. Phys. **85**, 3222 (1999). https://doi.org/10.1063/1.369664
3. Y. Lv, Z. Lin, T. Corrigan, J. Zhao, Z. Cao, L. Meng, C. Luan, Z. Wang, H. Chen, J. Appl. Phys. **109**, 074512 (2011). https://doi.org/10.1063/1.3569594
4. D. Marcon, J. Viaene, P. Favia, H. Bender, X. Kang, S. Lenci, S. Decoutere, Microelectron. Reliab. **52**, 2188 (2012). https://doi.org/10.1016/j.microrel.2012.06.052
5. D. Yan, H. Lu, D. Cao, D. Chen, R. Zhang, Y. Zheng, Appl. Phys. Lett. **97**, 153503 (2010). https://doi.org/10.1063/1.3499364
6. Z. Liu, G. Ng, S. Arulkumaran, Y. Maung, H. Zhou, Appl. Phys. Lett. **98**, 163501 (2011). https://doi.org/10.1063/1.3573794
7. J. Zhu, X. Ma, B. Hou, W. Chen, Y. Hao, Appl. Phys. Lett. **104**, 153510 (2014). https://doi.org/10.1063/1.4871802
8. D. Qiao, L. Yu, S. Lau, J. Redwing, J. Lin, H. Jiang, J. Appl. Phys. **87**, 801 (2000). https://doi.org/10.1063/1.371944
9. M. Rezau, H. Khan, H. Nakayama, T. Detchprohm, K. Hiramatsu, N. Sawaki, Solid State Electron. **41**, 287 (1997). https://doi.org/10.1016/S0038-1101(96)00231-6
10. L. Zhou, A. Ping, K. Boutros, J. Redwing, I. Adesida, Electron. Lett. **35**, 745 (1999). https://doi.org/10.1049/el:19990489
11. E. Arslan, Ş. Altındal, S. Özçelik, E. Ozbay, J. Appl. Phys. **105**, 023705 (2009). https://doi.org/10.1063/1.3068202
12. H. Kim, D. Lee, H. Myung, Korean J. Mater. Res. **26**, 412 (2016). https://doi.org/10.3740/MRSK.2016.26.8.412
13. R. Tung, Mater. Sci. Eng., R **35**, 1 (2001). https://doi.org/10.1016/S0927-796X(01)00037-7
14. D. Seghier, H. Gislason, Phys. Scr. **T101**, 230 (2002). https://doi.org/10.1238/Physica.Topical.101a00230
15. M. Khan, H. Nakayama, T. Detchprohm, K. Hiramatsu, N. Sawaki, Solid State Electron. **41**, 287 (1997). https://doi.org/10.1016/S0038-1101(96)00231-6
16. D. Donoval, A. Chvála, R. Šramatý, J. Kováč, E. Morvan, Ch. Dua, M. DiForte-Poisson, P. Kordoš, J. Appl. Phys. **109**, 063711 (2011). https://doi.org/10.1063/1.3560919
17. E. Monroy, F. Calle, J. Pau, F. Sánchez, E. Muñoz, F. Omnès, B. Beaumont, P. Gibart, J. Appl. Phys. **88**, 2081 (2000). https://doi.org/10.1063/1.1305838
18. J. Ren, D. Yan, Y. Zhai, W. Mou, X. Gu, Microelectron. Reliab. **61**, 82 (2016). https://doi.org/10.1016/j.microrel.2015.11.005
19. A. Belyaev, N. Boltovets, V. Ivanov, V. Klad'ko, R. Konakova, Y. Kudrik, A. Kuchuk, V. Milenin, Y. Sveshnikov, V. Sheremet, Semiconductors **42**, 689 (2008). https://doi.org/10.1134/S1063782608060092
20. H. Hasegawa, O. Susumu, J. Vac. Sci. Technol., B **20**, 1647 (2002). https://doi.org/10.1116/1.1491539